Robust automotive radar interference mitigation using multiplicative-adaptive filtering and Hilbert transform

Budiman Putra Asmaur Rohman[1,2], Arief Suryadi Satyawan[1,2,3], Dayat Kurniawan[1], Ratna Indrawijaya[1], Chaeriah Bin Ali Wael[1,4], Nasrullah Armi[1,2]

[1]Research Center for Telecommunication, National Research and Innovation Agency (BRIN), Bandung, Indonesia
[2]School of Electrical Engineering, Telkom University, Bandung, Indonesia
[3]Department of Electrical Engineering, Nurtanio University, Bandung, Indonesia
[4]Institut d'Électronique de Microélectronique et de Nanotechnologie, Université Polytechnique Hauts-de-France, Valenciennes, France

Article Info

ABSTRACT

Radar is one of the sensors that have significant attention to be implemented in an autonomous vehicle since its robustness under many possible environmental conditions such as fog, rain, and poor light. However, the implementation risks interference because of transmitting and/or receiving radar signals from/to other vehicles. This interference will increase the floor noise that can mask the target signal. This paper proposes multiplicative-adaptive filtering and Hilbert transform to mitigate the interference effect and maintain the target signal detectability. The method exploited the trade-off between the step-size and sidelobe effect on the least mean square-based adaptive filtering to improve the target detection accuracy, especially in the long-range case. The numerical analysis on the millimeter-wave frequency modulated continuous wave radar with multiple interferers concluded that the proposed method could maintain and enhance the target signal even if the target range is relatively far from the victim radar.

Corresponding Author:

Budiman Putra Asmaur Rohman
Research Center for Telecommunication, National Research and Innovation Agency (BRIN)
KST Samaun Samadikun, Sangkuriang Street, Dago, Coblong, Bandung, Indonesia
Email: budi057@brin.go.id

1. INTRODUCTION

Autonomous vehicles have become a hot topic in recent years. The sensor, as the key component of autonomous driving, needs robust data processing so that it can provide accurate sensing and understanding of the environment surrounding the vehicle. One of the sensors that are mostly applied in autonomous vehicles is radar. This sensor has distinctive advantages compared with other possible sensors such as camera, lidar, and ultrasound [1]. For example, this sensor is reliable facing rainy and foggy environments that are the limits of the camera sensor, and this radar is also more economical than lidar technology. The radar also can measure the range and speed simultaneously [2], [3]. One radar technology commonly applied in autonomous vehicles is frequency modulation continuous wave (FMCW) radar. The FMCW automotive radar is easily generated using a voltage-controlled oscillator (VCO), and its received echoes have a narrow frequency band after the signal processing step. Those characteristics make it an affordable option for customers and a widely available choice in the current market, especially for autonomous vehicles.

With the rising number of automotive radars being utilized on roads, the level of mutual interference between these radars is likely to intensify. Due to the high-duty cycle of radar systems, the possibility of interference among vehicles is increased. Radar-to-radar interference may present even in

simple road scenarios where vehicles travel in their respective lanes. This interference lowers the sensitivity of the radar instrument, potentially resulting in a ghost target, increased noise floor, masked weak targets, or reduced probability of target detection. Thus, many efforts by researchers have been conducted to address this issue.

In the case of radar waveform generation, some approaches have been introduced to suppress radar interference, as follows. Kitsukawa *et al.* [4] proposed FMCW radar with noise-like frequency in every cycle by resetting the parameter of the chirp. By using these strategies, partial interferences would be reduced. However, the fast Fourier transform (FFT), which is typically utilized, would be inapplicable for the fast Doppler processing due to these randomized repeat intervals. The chaotic sequences [5] and pseudo-random noise signals [6] radars are introduced to mitigate the automotive radar mutual interferences. However, a high sampling rate is typically needed to raise the price of the radar systems. Phase-modulated FMCW radar systems with orthogonal or random sequences were proposed in this method [7], [8], high correlation peaks are typically produced by the scattered signals from transmitted signals. However, following the decoding process, the uncorrelated interferences spread and the noise floor increased.

Several advanced signal processing methods have also been proposed to tackle this interference problem. The interference of array-based radar was suppressed by removing the signal from the direction of arrival of the interference [9]–[11]. However, these methods might lessen target signals that are reflected from the same direction as the interferences. The interference is first identified using a threshold before being suppressed by time windowing [12]. To decompose the output signal of FMCW radar, an iterative modified technique based on empirical mode decomposition is proposed in [13], while in [14], the wavelet denoising method was applied. Since those approaches assume that the interferences are sparse, their performances would degrade with increasing the proportion of contaminated samples in the recorded radar signal. Neemat *et al.* [15] proposed the use of Burg-based method to reconstruct the cut-out region in the frequency domain, which is indicated as interference. However, as the cut-out zone in the signal increases, the accuracy of the recovered signals decreases significantly. Recently some deep-learning approaches have been used for interference mitigation of FMCW radars, such as using recurrent neural network [16], convolutional neural network [17], [18], two-stage deep neural network [19], and autoencoder [20]. These methods seem promising to provide accurate results but for the training process, these methods often require an extensive dataset collected in various settings since the generality of those approaches needs to be confirmed thoroughly. The interference of FMCW automotive radar is mitigated by the constant false alarm rate (CFAR) method [21]. In this method, the CFAR detector is used to identify massive chirp-pulse-like interferences in the time-frequency domain, and subsequently the zeroing, amplitude correction, and signal extrapolation procedures are used. Though this method is superior to other existing methods, the method is relatively complex and time-consuming. The use of adaptive noise cancellation for automotive radar interference mitigation has been proposed in [22]. This method is computationally efficient, but there is a trade-off between the step size of updating algorithm and the sidelobe level of the signal, so the appropriate configuration is required.

In this paper, we propose a method to mitigate automotive radar interference in case the radar parameters between the victim and aggressor car are different. The proposed method uses multiplicative-adaptive filter and Hilbert transform. This method is an improved version of the existing method that uses the least-mean-squared-based adaptive filter, as in [22]. Our method applies multiple adaptive filters with different step sizes and applies Hilbert transform before processing the multiplication of signals. This multiplication will enhance the coherent filtered signal that may contain the target signal. The method addresses the trade-off between the adaptive filter's step size and the output signal's sidelobe. In this issue, the big step size will enhance the output's signal-to-interference-and-noise ratio (SINR), but the sidelobe is also increased. This configuration will decrease the accuracy of detection. In contrast, when the step size became very small, the sidelobe would decrease, but the SINR of the output signal became lower. Thus, the idea of this paper is that by combining those configurations and extracting the coherent signal only, the target signal can be enhanced.

The remainder of this paper is organized as follows. Section 2 briefly explains the proposed system architecture. Followed by the result and discussion in section 3. Finally, the conclusion of this study is described in Section 4.

2.   PROPOSED INTERFERENCE MITIGATION METHOD
2.1. Scenario on the automotive radar interference
Figure 1 shows the scenario of automotive radar in case of mutual interference presence. Mutual interference happens when two or more cars or vehicles face each other on the road, as depicted in Figure 1(a). The radar in the victim's car receives two types of signals: target echo signals and interference signals from the aggressor's car. The target echo signal, reflected by the target, is the desired signal for the

receiver and is primarily used for ranging and positioning. Depending on whether the waveform utilized by the aggressor and victim radar are the same, interference signals in automotive radar may be divided into two groups. This study focuses on the case of automotive radars with distinct parameters. The received signal in this scenario can be illustrated in Figures 1(b) and 1(c). Figure 1(b) depicts the received signal when there is no interference, while Figure 1(c) shows the condition when there is interference from an aggressor radar with different chirp parameters.
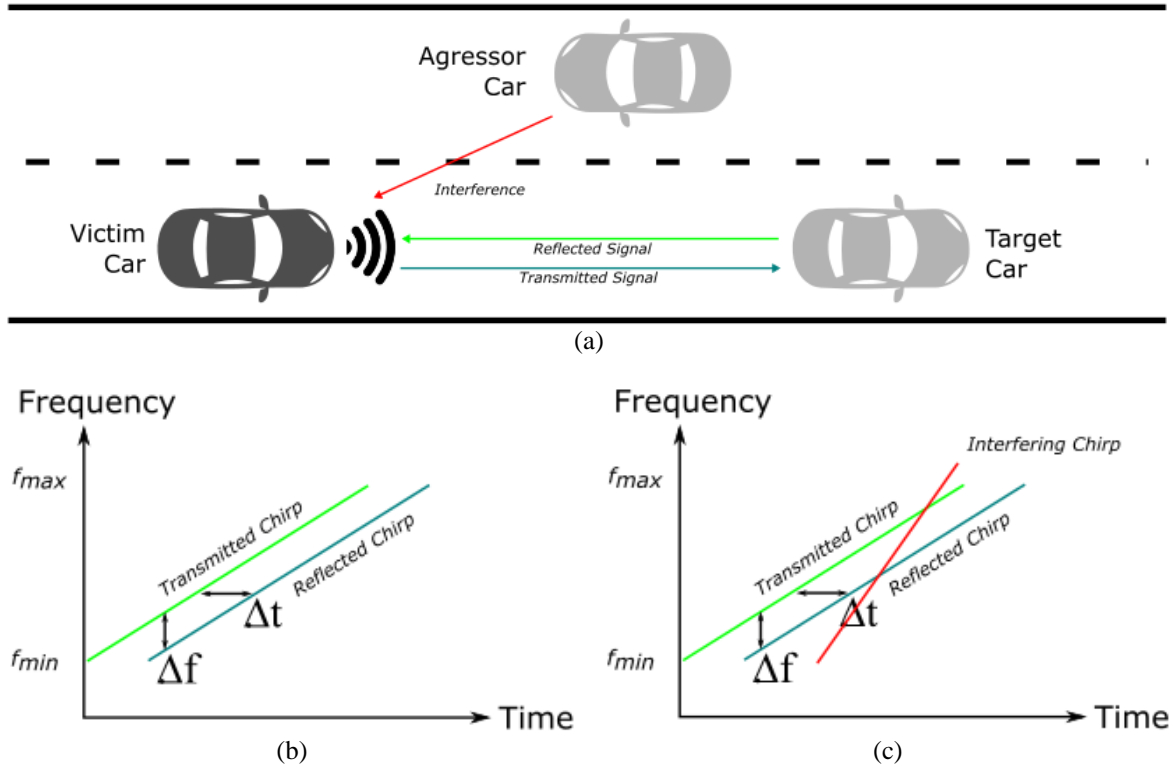
Figure 1. The scenario of automotive radar: (a) traffic situation, (b) received signal of FMCW radar without interference, and (c) with interference with different parameters

2.2. Proposed method

This study focuses on the quadrature receiver automotive FMCW radar, which has a general architecture illustrated in Figure 2. The radar transmits a signal with a linearly swept frequency between a start and stop frequency. When the signal reflects off a target at a distance (d), it incurs a delay (t), which is the sum of the travel time of the outgoing transmit signal from the radar to the target and the return time of the reflected signal back to the radar. This time difference results in a shift in the received signal. Given that the VCO changed frequencies during t, the signal's frequency when it reaches the receiver will be different from the transmit frequency. With the help of this frequency shift, the absolute distance can be calculated accurately. The calculation of distance d is as (1),

$$d = c.\frac{\Delta t}{2} \tag{1}$$

where

$$\Delta t = \frac{\Delta f}{m} \tag{2}$$

and m is the rate of the frequency ramp in Hz/s.

A power amplifier (PA) enhances the signal fed from the VCO output. The PA output signal is then separated into a power signal and a local oscillator (LO) signal using a splitter. The power signal is

transmitted to a transmitting antenna (Tx), while a receiving antenna (Rx) receives the signal and feeds it to a low-noise amplifier (LNA). The mixer down-converts the output of the LNA with the LO signal generated by the splitter. This process outputs the in-phase signals. Another mixer is employed to down-convert the output of LNA using a 90° phase-shift version of VCO output signal to produce quadrature signals. The down-converted signal is then filtered and amplified for measurement. Through a signal processing step, instead of object distance, the velocity also can easily be measured through the change in distance over time.
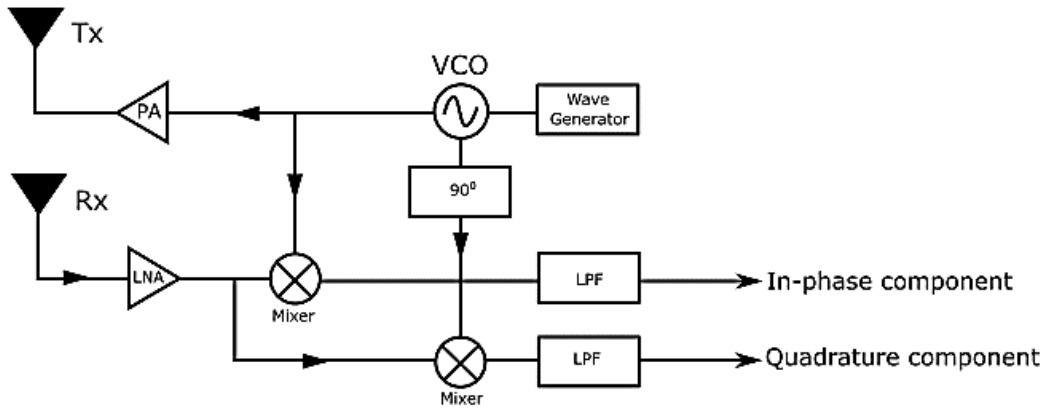
Figure 2. General design of FMCW radar system

FMCW radar transmitted signal whose frequency increases linearly, s_T, can be expressed as (3) [23], [24].

$$s_T = Re\left\{e^{j2\pi\left(f_c+\frac{a}{2t}\right)t}\right\} = \cos\left(2\pi\left(f_c + \frac{a}{2}t\right)t\right) \tag{3}$$

f_c is the center frequency and a is the chirp rate of ramp signal. The signal received from several targets can be expressed as (4).

$$s_R(t) = \sum_{m=1}^{N} A_m s_T(t - \tau_m) + w(t) \tag{4}$$

N is the number of targets, A_m, τ_m are the attenuation and time delay from the m^{-th} target, respectively, and $w(t)$ is the additive noise signal. Then we get the intermediate frequency (IF) or beat signal after mixing process with the LO signal given by (15),

$$s_b(t) = \sum_{m=1}^{N} A_m e^{j2\pi(f_{bm}\cdot t+\phi_m)} + n(t) \tag{5}$$

where f_{bm} is the beat frequency and ϕ_m denoted phase of the signal, while $n(t)$ is the noise. The maximum distance from the target R_{max} determine the maximum beat frequency f_{bmax},

$$f_{bmax} = \frac{2R_{max}}{c} \cdot \frac{B}{T} \tag{6}$$

where B is the frequency bandwidth, T is the sweep duration.

Figure 3 shows the proposed signal processing method. After the FFT operation on the s_b signal to calculate the frequency shift, we apply our proposed method, multiplicative-adaptive filtering, and Hilbert transform, where the general design can be seen in Figure 3(a). The method uses multiple individual adaptive filters adapted from [22]. In this individual adaptive filter, as shown in Figure 3(b), it is presumable that interference in the positive and negative halves of the frequency spectrum corresponds where only the positive half contains the target signal. The positive and negative halves of the FFT are then fed into the primary ($i_p[k] + e[k]$) and reference ($i_n[k]$) channels, respectively. $e[k]$ represents the beat signal due to the

target existence, $i_p[k]$ is the interference in the positive and $i_n[k]$ is negative half of FFT, with k is bin number. When the adaptive filter generates an optimal estimation of $ip[k]$ from a reference input $in[k]$, the $ip[k]$ can be removed producing an optimal estimation of $e[k]$ represented by $\epsilon[k]$ so that:

$$\epsilon = e + i_p - y = e + i_p - w_o^T i_n(k) \tag{7}$$

where $i_n(k)$ is L-by-1 adaptive filter input vector with L is the filter length, w_0 is the L-by-1 tape-coefficient vector, and $y[k]$ represents the output.
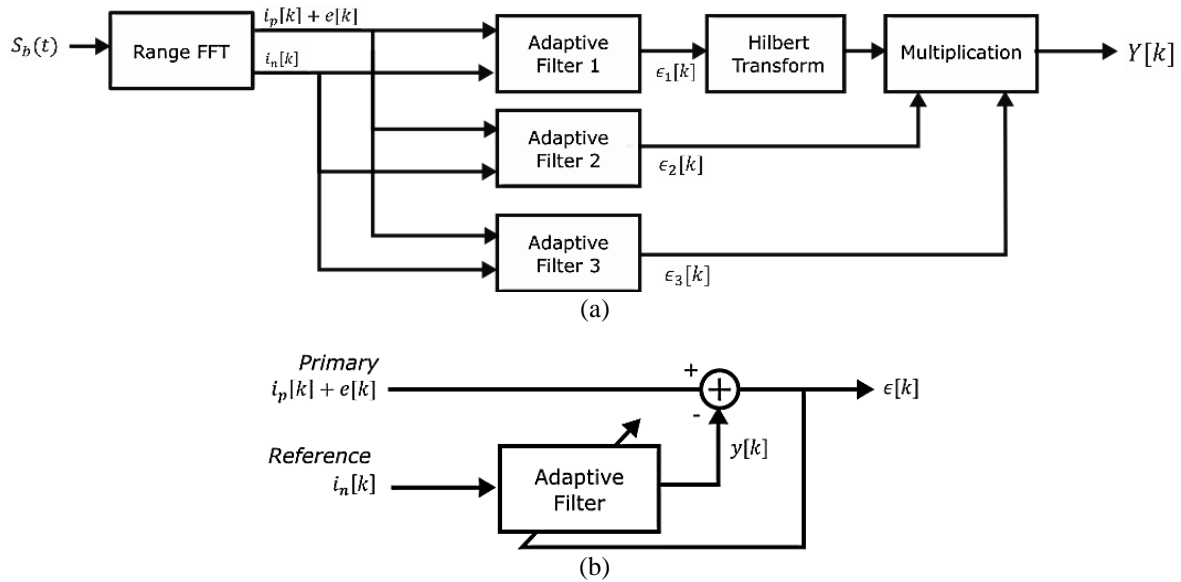
Figure 3. Design of (a) overall proposed method and (b) individual adaptive filter

Then, by using statistical expectation on both sides, we have (8) and (9).

$$E[\epsilon^2] = E[e]^2 + E\{[i_p - w_o^T i_n(k)]^2\} \tag{8}$$

$$\min\{E[(\epsilon - e)^2]\} = \min\{E[(i_p - y)^2]\} \tag{9}$$

The least mean squared method is employed to solve for the minimum of $E[\epsilon^2]$ by changing the filter taps w to w_o with a step size Δw step by step. Therefore, the filter be computed as (10) to (12),

$$y[k] = w^T[k]i_n[k] \tag{10}$$

$$\epsilon[k] = e[k] + i_p[k] - y[k] \tag{11}$$

$$w[k + 1] = w[k] + \Delta w i_n[k]\epsilon * [k] \tag{12}$$

with Δw is step size that determine filter's convergence speed and stability.

The signals from adaptive filters with the largest step size ($n = 1$) are then computed by using Hilbert transform. This process is needed to make a smoother shape on the signal time series that may contain the target signal. The Hilbert transform is able to characterize the instantaneous amplitude and frequency attributes of time domain signal. The instantaneous amplitude is the complex Hilbert transform's amplitude, and the instantaneous frequency is the rate at which the instantaneous phase angle changes [25], [26]. One of the uses is to extract the signal envelope as in [27]. The analytic signal A_s is expressed by using the Hilbert transform pair, as (13),

$$A_s(t) = x(t) + iH\{x(t)\} \tag{13}$$

where

$$H\{x(t)\} = \frac{1}{\pi} P.V. \int_{-\infty}^{\infty} \frac{x(\tau)}{\tau - t} d\tau \qquad (14)$$

with $x(t)$ is the any signal, $i = \sqrt{-1}$, $H\{x(t)\}$ is the Hilbert transform, and $P.V.$ means the Cauchy principal value. After transforming to the analytic signal and extracting the signal envelope, the signal is then multiplicated with two remaining signals concurrently. Considering that the output of the individual adaptive filter is $\epsilon_j[k]$ where j is the index of the individual adaptive filter, the signal after the multiplication process can be described by (15).

$$Y[k] = H\{\epsilon_1[k]\} \cdot \epsilon_2[k] \cdot \epsilon_3[k] \qquad (15)$$

3. RESULTS AND DISCUSSION
3.1. Numerical analysis setup

To evaluate the proposed method, we conducted numerical analyses using an FMCW radar with a frequency of 76 GHz. The chirp bandwidth is 300 MHz with duration and rate is 51.2 us, and 5.86 MHz/us, respectively. We used a sampling rate of 40 MHz, a low-pass filter bandwidth of 10 MHz, and an FFT size of 2,048. The gain of the receiver LNA was 40 dB. For simplicity, we set the radar cross-section (RCS) of the radar target to 1, and there were two targets with an overall interference number of three. The complete scenario of the numerical evaluation is shown in Table 1 with center frequency f_c, chirp duration T, chirp rate μ, distance d, and normalized RCS σ. In this study, we made the distance d of the target as a variable to further evaluate the proposed method's performance.

Table 1. Scenario of signal components and their parameters

No	Signal	Parameters	Value	Unit
1	Target 1 (T1)	d	35 (variable)	meter
		σ	1	dBsm
2	Target 2 (T2)	d	100 (variable)	meter
		σ	4	dBsm
3	Interference 1 (I1)	f_c	76	GHz
		T	10	μs
		μ	30	MHz/μs
		d	10	meter
4	Interference 2 (I2)	f_c	76	GHz
		T	8	Us
		μ	37.5	MHz/μs
		d	30	meter
5	Interference 3 (I3)	f_c	76.1	GHz
		μ	0	MHz/μs
		d	40	meter

3.2. Result of the numerical analysis

The simulated received signal is shown in Figure 4, where on the left and right side is the signal containing the target signal without and with interference signal, respectively. In Figures 4(a) and 4(b), we can see the signal before mixing. The interference makes the target signal unclear. Then, from the Fourier transform of the received signal, as shown in Figures 4(c) and 4(d), the beat signals were significantly impaired by the interference resulting in the inaccuracy of the target detection. When the interference is plotted in the time domain, it resembles pulse signals, as shown in Figures 4(e) and 4(f).

Figure 5 shows the three outputs of individual filters with step size Δw of $\frac{2}{20 \times P}$, $\frac{2}{50 \times P}$, $\frac{2}{70 \times P}$, respectively, as shown in Figures 5(a) to (c), and one output of our proposed filter that employ those three step sizes as shown in Figure 5(d). The selection of step size was taken based on evaluating the effect of every step size on the signal quality. The three steps size was selected as the minimum number of configurations that produce an optimum signal based on the numerical evaluation on every observed case. This figure is for the case of two targets in the range of 35 and 100 m. Figure 5(a) has the largest step size, and the third is the smallest one, as shown in Figure 5(c). As concluded in [22], a large step size Δw will be produced in the final filter solution deviating from the optimum Wiener filter. When Δw was decreased, the side lobes disappeared but target signal strength became lower. This conclusion can be confirmed in

Figure 5(a), where both targets have a wide sidelobe but in Figure 5(c), T2 is partly masked by the interference. Our proposed method combines those three step sizes with the advanced processing illustrated in Figure 3.
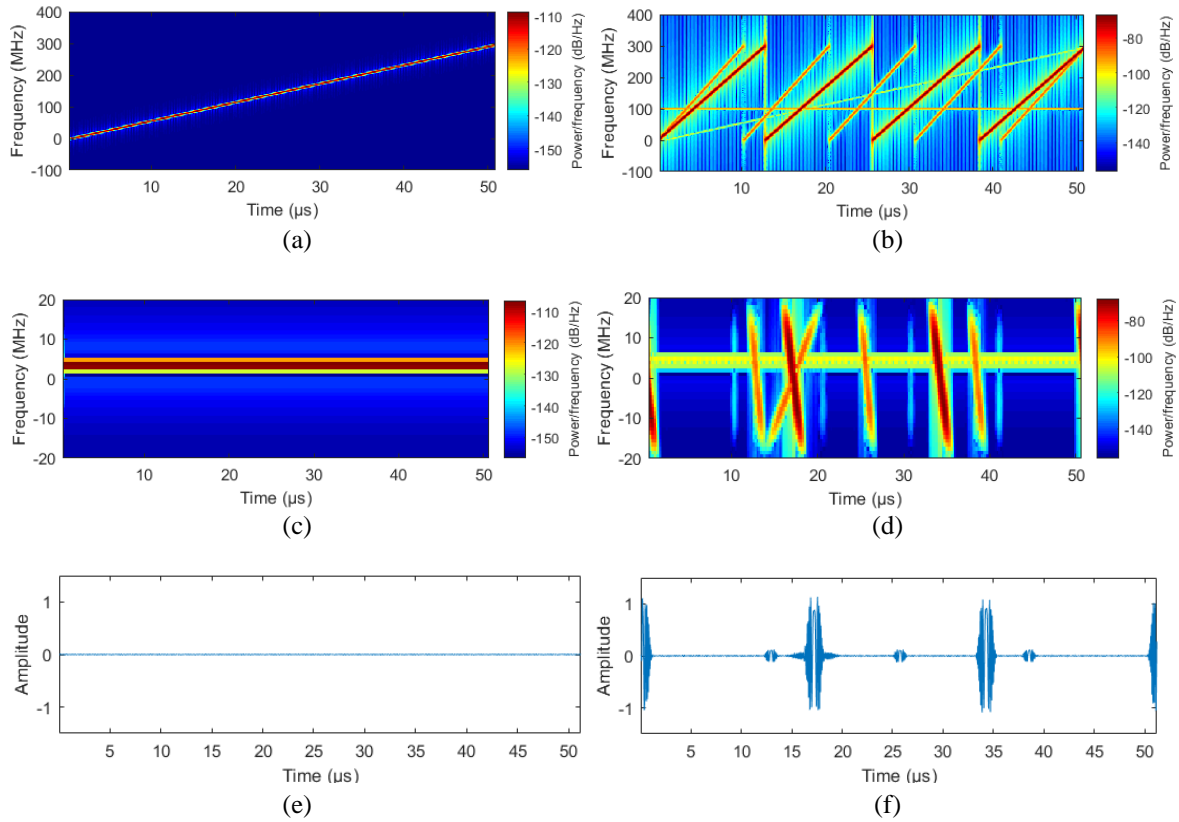

(a)

(b)

(c)

(d)

(e)

(f)

Figure 4. The signal received by victim radar, without and with interference, respectively: (a) and (b) the received signal before mixing, (c) and (d) the received signal after mixing, (e) and (f) the time domain of received signal
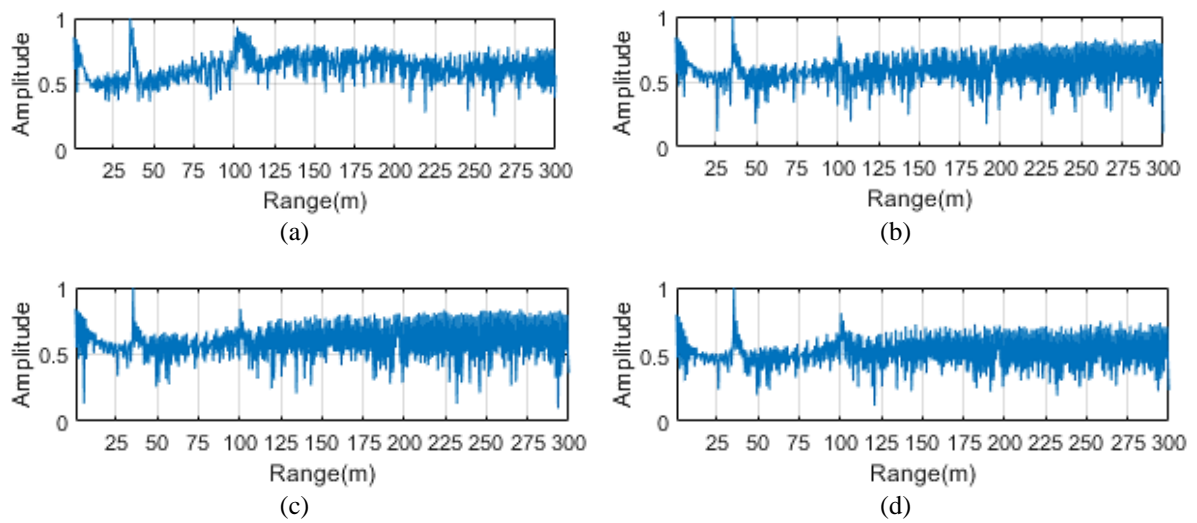

(a)

(b)

(c)

(d)

Figure 5. Result of processing using the individual filter with step size Δw (a) $\frac{2}{20 \times P}$, (b) $\frac{2}{50 \times P}$, (c) $\frac{2}{70 \times P}$, and (d) using the multiplicative-adaptive filter

3.3. Comparison of the method

To see the comparison of the proposed method to the existing methods, we observe the same target cases with the existing method in [22] that proposed the use of an adaptive filter with step size $\Delta w = \frac{2}{100 \times P}$. The result of the comparison as shown in Figure 6. In Figure 6(a), the target signals T1 and T2 were buried because of the interferences. However, in both Figures 6(b) and 6(c), the T1 signal can be detected by both methods. Meanwhile, the interference almost completely buries the signal T2, and the existing method introduced in [22] cannot maintain this signal detectability. This condition can be solved by employing our proposed method. As shown in Figure 6(c), the T2 signal can be reconstructed at a certain level. This result has been confirmed by qualitative analysis of the SINR levels with a window with a width of 20 reference cells and six guard cells shown in Table 2. The proposed method employed multiple step sizes of adaptive filter and extracted the coherent signal that will improve the clarity and detectability of the target signal even if placed in the long range.

(a)

(b)

(c)
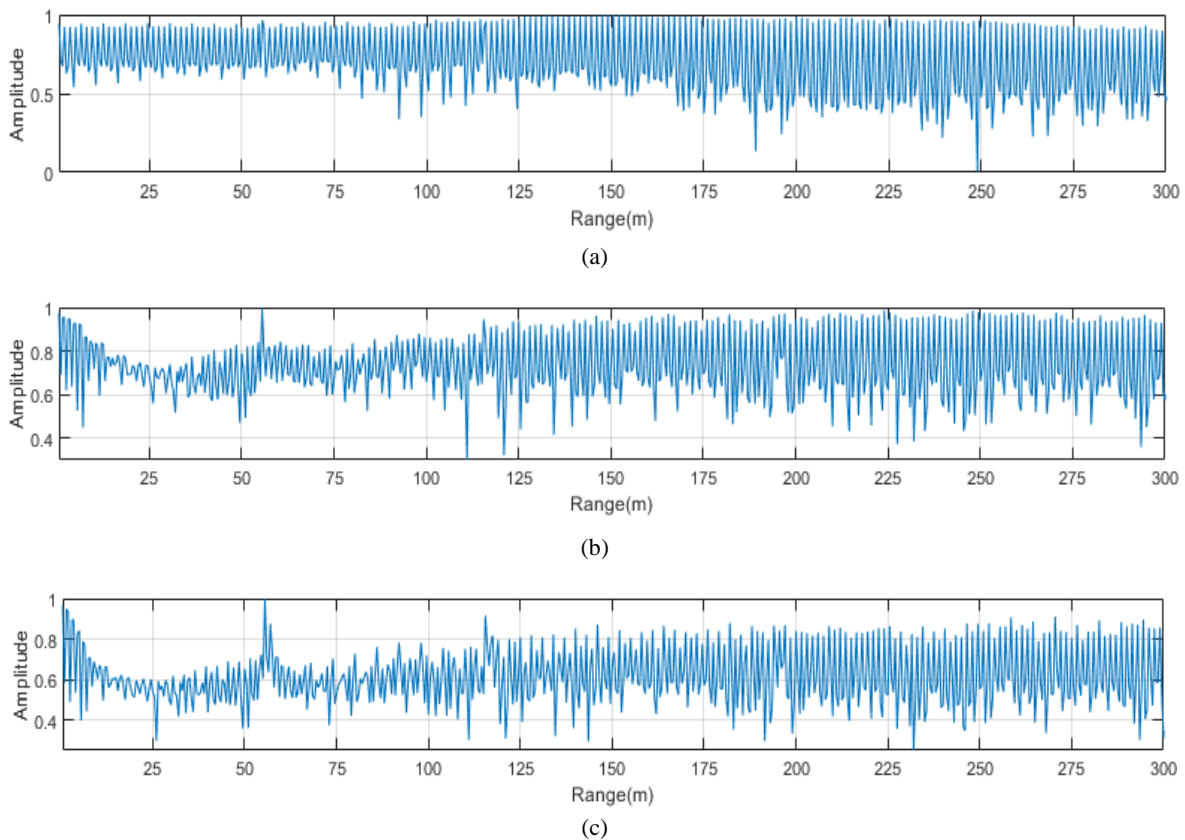
Figure 6. Comparison of mitigation result in case of T1 and T2 in the range of 55 and 115 m, respectively:
(a) before mitigation, (b) after baseline mitigation, and (c) after proposed method

Table 2. Comparison of the SINR before and after mitigation

Target	SINR (dB)		
	Before mitigation	Baseline method	Proposed method
T1 (55 m)	6.3	15.5	41.2
T2 (115 m)	1.9	10.9	21.9

Figure 7 compares the range-Doppler map before and after mitigation in the case of one target in the range of 70 m with interference. Figure 7(a) shows the map without any interferences. It can be observed that interference can mask the detected object on the map as shown in Figure 7(b). The baseline mitigation method [22] can suppress the interference, as shown in Figure 7(c), but the proposed method can enhance the object's signature with a better performance, as shown in Figure 7(d).
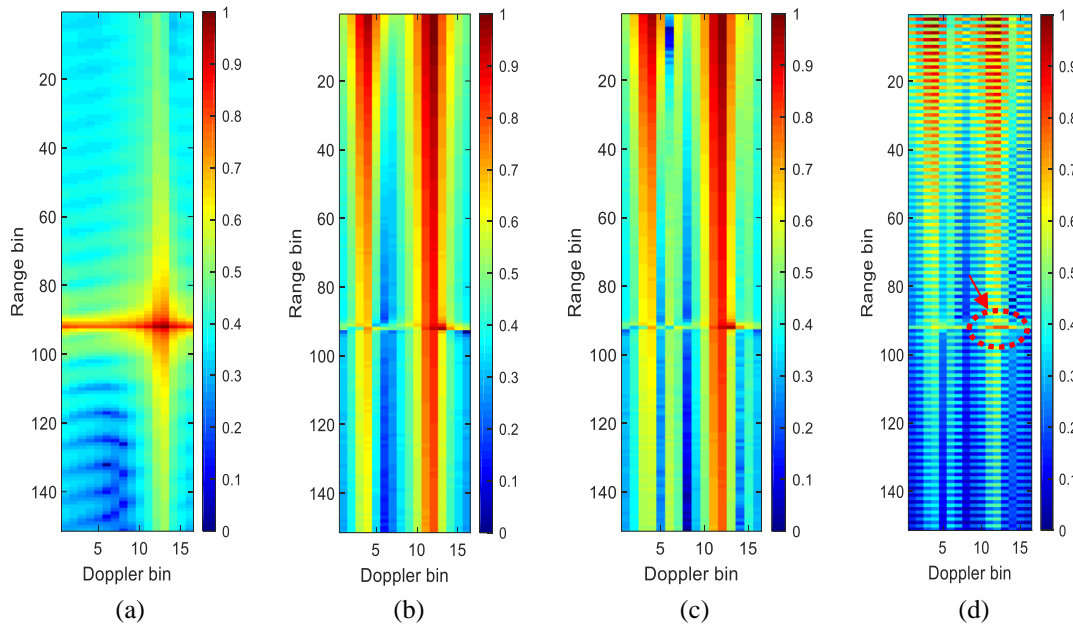
Figure 7. Comparison range Doppler map in case of (a) without interference (b) with interference,
(c) after mitigation with baseline method, and (d) after mitigation with proposed method

4. CONCLUSION

This paper presents our proposed method to mitigate automotive radar interference using a combination of multiplicative-adaptive filtering and Hilbert transform. Our method effectively resolves the trade-off between the sidelobe level and the step size of the LMS-based adaptive filter aiming the detection performance improvement. We conducted numerical analysis on a simulated millimeter-wave FMCW radar, demonstrating that our method could suppress the interferences and enhance the system's target detection capabilities, particularly for targets at longer ranges. This improvement is especially critical for autonomous vehicles, where expanding the maximum detected range is essential for reducing the risk of accidents. By effectively mitigating interference from automotive radar, our proposed method can elevate the functionality of radar systems, making them more reliable and accurate.

REFERENCES

[1] A. Herrmann, W. Brenner, and R. Stadler, *Autonomous driving: How the driverless revolution will change the world*. Emerald Publishing Limited, 2018. doi: 10.1108/9781787148338.

[2] D. G. Yang *et al.*, "Intelligent and connected vehicles: Current status and future perspectives," *Science China Technological Sciences*, vol. 61, no. 10, pp. 1446–1471, Sep. 2018, doi: 10.1007/s11431-017-9338-1.

[3] J. Gamba, *Radar signal processing for autonomous driving*. Singapore: Springer Singapore, 2020. doi: 10.1007/978-981-13-9193-4.

[4] Y. Kitsukawa, M. Mitsumoto, H. Mizutani, N. Fukui, and C. Miyazaki, "An interference suppression method by transmission chirp waveform with random repetition interval in fast-chirp FMCW radar," in *2019 16th European Radar Conference (EuRAD)*, 2019, pp. 165–168.

[5] E. Gambi, F. Chiaraluce, and S. Spinsante, "Chaos-based radars for automotive applications: Theoretical issues and numerical simulation," *IEEE Transactions on Vehicular Technology*, vol. 57, no. 6, pp. 3858–3863, Nov. 2008, doi: 10.1109/TVT.2008.921632.

[6] Z. Xu and Q. Shi, "Interference mitigation for automotive radar using orthogonal noise waveforms," *IEEE Geoscience and Remote Sensing Letters*, vol. 15, no. 1, pp. 137–141, Jan. 2018, doi: 10.1109/LGRS.2017.2777962.

[7] F. Uysal, "Phase-Coded FMCW automotive radar: System design and interference mitigation," *IEEE Transactions on Vehicular Technology*, vol. 69, no. 1, pp. 270–281, Jan. 2020, doi: 10.1109/TVT.2019.2953305.

[8] E. H. Kim and K. H. Kim, "Random phase code for automotive MIMO radars using combined frequency shift keying-linear FMCW waveform," *IET Radar, Sonar and Navigation*, vol. 12, no. 10, pp. 1090–1095, Oct. 2018, doi: 10.1049/iet-rsn.2018.5075.

[9] J. Bechter, M. Rameez, and C. Waldschmidt, "Analytical and experimental investigations on mitigation of interference in a DBF MIMO radar," *IEEE Transactions on Microwave Theory and Techniques*, vol. 65, no. 5, pp. 1727–1734, May 2017, doi: 10.1109/TMTT.2017.2668404.

[10] I. Artyukhin, V. Ermolaev, A. Flaksman, A. Rubtsov, and O. Shmonin, "Development of effective anti-interference primary signal processing for mmWave automotive radar," Nov. 2019. doi: 10.1109/EnT47717.2019.9030561.

[11] M. Rameez, M. Dahl, and M. I. Pettersson, "Adaptive digital beamforming for interference suppression in automotive FMCW radars," in *2018 IEEE Radar Conference, RadarConf 2018*, Apr. 2018, pp. 252–256. doi: 10.1109/RADAR.2018.8378566.

[12] T. Nozawa *et al.*, "An anti-collision automotive FMCW radar using time-domain interference detection and suppression," in *IET Conference Publications*, 2017, vol. 2017, no. CP728. doi: 10.1049/cp.2017.0366.

[13] J. Wu, S. Yang, W. Lu, and Z. Liu, "Iterative modified threshold method based on EMD for interference suppression in FMCW radars," *IET Radar, Sonar and Navigation*, vol. 14, no. 8, pp. 1219–1228, Jun. 2020, doi: 10.1049/iet-rsn.2020.0092.

[14] S. Lee, J. Y. Lee, and S. C. Kim, "Mutual interference suppression using wavelet denoising in automotive FMCW radar systems," *IEEE Transactions on Intelligent Transportation Systems*, vol. 22, no. 2, pp. 887–897, Feb. 2021, doi: 10.1109/TITS.2019.2961235.

[15] S. Neemat, O. Krasnov, and A. Yarovoy, "An interference mitigation technique for FMCW radar using beat-frequencies interpolation in the STFT domain," *IEEE Transactions on Microwave Theory and Techniques*, vol. 67, no. 3, pp. 1207–1220, Mar. 2019, doi: 10.1109/TMTT.2018.2881154.

[16] J. Mun, S. Ha, and J. Lee, "Automotive radar signal interference mitigation using RNN with self attention," in *ICASSP, IEEE International Conference on Acoustics, Speech and Signal Processing - Proceedings*, May 2020, vol. 2020-May, pp. 3802–3806. doi: 10.1109/ICASSP40776.2020.9053013.

[17] J. Rock, M. Toth, P. Meissner, and F. Pernkopf, "Deep interference mitigation and denoising of real-world FMCW radar signals," in *2020 IEEE International Radar Conference, RADAR 2020*, Apr. 2020, pp. 624–629. doi: 10.1109/RADAR42522.2020.9114627.

[18] J. Rock, W. Roth, M. Toth, P. Meissner, and F. Pernkopf, "Resource-efficient deep neural networks for automotive radar interference mitigation," *IEEE Journal on Selected Topics in Signal Processing*, vol. 15, no. 4, pp. 927–940, Jun. 2021, doi: 10.1109/JSTSP.2021.3062452.

[19] S. Chen, J. Taghia, U. Kuhnau, N. Pohl, and R. Martin, "A two-stage DNN model with mask-gated convolution for automotive radar interference detection and mitigation," *IEEE Sensors Journal*, vol. 22, no. 12, pp. 12017–12027, Jun. 2022, doi: 10.1109/JSEN.2022.3173129.

[20] S. Chen, J. Taghia, T. Fei, U. Kühnau, N. Pohl, and R. Martin, "A DNN autoencoder for automotive radar interference mitigation," in *ICASSP, IEEE International Conference on Acoustics, Speech and Signal Processing - Proceedings*, Jun. 2021, vol. 2021-June, pp. 4065–4069. doi: 10.1109/ICASSP39728.2021.9413619.

[21] J. Wang, "CFAR-based interference mitigation for FMCW automotive radar systems," *IEEE Transactions on Intelligent Transportation Systems*, vol. 23, no. 8, pp. 12229–12238, Aug. 2022, doi: 10.1109/TITS.2021.3111514.

[22] F. Jin and S. Cao, "Automotive radar interference mitigation using adaptive noise canceller," *IEEE Transactions on Vehicular Technology*, vol. 68, no. 4, pp. 3747–3754, Apr. 2019, doi: 10.1109/TVT.2019.2901493.

[23] Y. S. Son, H. K. Sung, and S. W. Heo, "Automotive frequency modulated continuous wave radar interference reduction using per-vehicle chirp sequences," *Sensors (Switzerland)*, vol. 18, no. 9, p. 2831, Aug. 2018, doi: 10.3390/s18092831.

[24] J. J. Lin, Y. P. Li, W. C. Hsu, and T. S. Lee, "Design of an FMCW radar baseband signal processing system for automotive application," *SpringerPlus*, vol. 5, no. 1, pp. 1–16, Jan. 2016, doi: 10.1186/s40064-015-1583-5.

[25] S. Lawrence Marple, "Computing the discrete-time analytic signal via FFT," *IEEE Transactions on Signal Processing*, vol. 47, no. 9, pp. 2600–2603, 1999, doi: 10.1109/78.782222.

[26] Y.-W. Liu, "Hilbert transform and applications," in *Fourier Transform Applications*, InTech, 2012. doi: 10.5772/37727.

[27] B. P. A. Rohman, M. Nishimoto, and K. Ogata, "Material permittivity estimation using analytic peak ratio of air-coupled GPR signatures," *IEEE Access*, vol. 10, pp. 13219–13228, 2022, doi: 10.1109/ACCESS.2022.3147217.

BIOGRAPHIES OF AUTHORS

Budiman Putra Asmaur Rohman 🆔 📊 SC ☀ received a B.Eng. degree in engineering physics from Institut Teknologi Sepuluh Nopember, Indonesia, in 2009, an M. Eng, degree in computer science and electrical engineering, and a Ph.D. degree in human and environmental informatics, from Kumamoto University, Japan, in 2018 and 2021, respectively. Since 2015, he has been with National Research and Innovation Agency, Indonesia. In 2020, he was a visiting researcher at the Fraunhofer FHR, Germany. From 2021 to 2022, he was a researcher at Kumamoto University, Japan. Since 2022, he has been also with the School of Electrical Engineering, Telkom University, Indonesia. His research interests include signal processing, machine learning, radar, and embedded systems. He can be contacted at budi057@brin.go.id.

Arief Suryadi Satyawan 🆔 📊 SC ☀ has joined the Research Center for Electronics and Telecommunication, National Research and Innovation Agency since 1996. He received his bachelor's degree in electrical engineering from Universitas Jenderal Achmad Yani Bandung, Indonesia, in 2000. In 2007, he received his master's degree in electrical engineering from Institut Teknologi Bandung, Indonesia. He got his Ph.D. in computer and communication engineering from Waseda University, Japan, in 2019. His current research is on image and video processing, and video communication systems. He is a member of The Institute of Image Information and Television Engineers (ITE), Japan, and the Information Processing Society of Japan (IPSJ). He can be contacted at arief.suryadi@akane.waseda.jp.

Dayat Kurniawan received a master's degree in electrical engineering from the Bandung Institute of Technology, Bandung, Indonesia, in 2019. His research interests cover the areas of radar signal processing, wireless communication, and embedded systems. He is currently working as a researcher at the Research Center for Telecommunications, National Research and Innovation Agency. He can be contacted at daya004@brin.go.id.

Ratna Indrawijaya received a B.Eng. degree in electronics engineering from Institut Teknologi Sepuluh Nopember Surabaya, Indonesia, in 2003, and an M.Eng. degree in telecommunication engineering from Institut Teknologi Bandung, Indonesia, in 2013. Since 2005 he has been with the Research Center for Electronics and Telecommunications, Indonesian Institute of Science in Bandung, Indonesia. He studies real-time signal processing, software-defined radio, FPGA design, and radar systems. He worked on a THz wireless communication project from 2017 to 2020 with the Institute for Communications Technologies at Technische Universität Braunschweig in Germany. He is presently employed with the Research Center for Telecommunication of Indonesia's National Research and Innovation Agency. His current research projects involve MIMO radar, wireless data communications for UAVs, and reconfigurable computing devices, mainly FPGAs. He can be contacted at ratna.indrawijaya@brin.go.id.

Chaeriah Bin Ali Wael received her master's in electrical engineering from Institut Teknologi Sepuluh Nopember, Surabaya, Indonesia. She joined the Research Center for Electronics and Telecommunication, LIPI in 2015 as a junior researcher. Currently, she is pursuing her Ph.D. degree in 5G enabling technology for Intelligent Transportation Systems at Institut d'Électronique de Microélectronique et de Nanotechnologie (IEMN), Université Polytechnique Hauts-de-France (UPHF), France. Her research interests include wireless communications, signal processing, and machine learning. She can be contacted at chae005@brin.go.id.

Nasrullah Armi received a Master of Engineering degree from the Department of Knowledge-based Information Engineering at Toyohashi University of Technology, Japan, in 2004. Then in 2013, he received his Ph.D. from the Department of Electrical and Electronic Engineering at Universiti Teknologi Petronas, Malaysia. Signal Processing, Wireless Communication and Networks are among his research interests. He presented at international conferences and published scientific articles in peer-reviewed journals. He shared his expertise as a scientific reviewer for international impact journals and as a member of the Scientific Committee for International Conferences. He is currently employed as a researcher at the National Research and Innovation Agency's Research Center for Telecommunication. He can be contacted at nasr004@brin.go.id.